pipe wall temperature at points of attachment of bundles from body i in K; T_{wn} pipe wall temperature at point of attachment for bundle n in K; $(\sigma_i)_n$ and σ_i thermal conductivities of bundle n and all bundles from body i in W/K; σ_{ij} thermal conductivity between bodies i and j in W/K; σ_{ci}, σ_Σ, σ_{cw} thermal conductivities from case to body i and total and radiative conductivities from case to pipe in W/K; α_c convective heat-transfer coefficient between pipe and coolant in $W/m^2 \cdot K$; α_r radiative heat-transfer coefficient between case and pipe in $W/m^2 \cdot K$; λ pipe material thermal conductivity in W/m·K; c specific heat of helium at constant pressure in J/kg·K; q and q_r correspondingly densities of the total heat flux and radiative flux to the pipe in W/m^2; P_r heat flux along bundle r in W; M coolant mass flow rate in kg/sec; F tube cross section area in m^2; S_i and S_o inside and outside surface areas of pipe in m^2; L pipe length in m; $\bar{x} = x/L$ relative coordinate along pipe axis; $\bar{x}_r$ relative coordinate for bundle r attachment; R total number of bundles; N_i number of bundles cooling body i; J_i number of bodies linked by heat bridges to body i; δ_i relative error in calculating the temperature of body i by comparison with numerical result in %; δ_w mean relative error in heat exchanger temperature calculated numerically by comparison with temperature from (4) taken at ten equally separated points in %; $\delta(\bar{x} - \bar{x}_r)$ Dirac function.

LITERATURE CITED

1. M. Akamatsu, M. Taneda, Y. Ohtsu, et al., Adv. Cryog. Eng., 31, 559-566 (1986).
2. V. A. Romanenko, S. V. Tikhonov, S. I. Khankov, and N. K. Yagupova, Inzh.-Fiz. Zh., 56, No. 4, 617-625 (1989).
3. B. N. Yudaev, Heat Transfer [in Russian], Moscow (1981).
4. O. Ore, Graph Theory [Russian translation], Moscow (1980).
5. I. S. Zhitomirskii, A. V. Borisenko, L. A. Ishchenko, and V. A. Pestryakov, Heat and Mass Transfer V [in Russian], Minsk (1976), pp. 25-29.
6. I. S. Zhitomirskii and V. G. Romanenko, Hydrodynamics and Heat Transfer in Cryogenic Systems [in Russian], Kharkov (1974), Issue 4, pp. 23-28.
7. G. N. Dul'nev, Heat and Mass Transfer in Electronic Equipment [in Russian], Moscow (1984).
8. R. Siegel and D. Howell, Radiative Heat Transfer [Russian translation], Moscow (1975).

EXTERNAL HEAT TRANSFER IN POLYDISPERSED FLUIDIZED BEDS AT ELEVATED TEMPERATURES

V. A. Borodulya, Yu. S. Teplitskii, A. P. Sorokin, V. V. Matsnev, I. I. Markevich, and V. I. Kovenskii

UDC 66.096.5

The authors present results of a theoretical and experimental study of heat transfer in polydispersed fluidized beds of coarse particles at temperatures up to 1273 K.

The technique of fluidization is traditionally widely used in chemical technology, metallurgy, oil processing, etc. Recently its sphere of application has been expanded into a number of new areas, amongst which the foremost is energetics. A prominent place is occupied by high-efficiency processes of combustion and gasification of solid fuel. One important problem arising in introducing fluidized technology into energetics is the need to design heat exchangers, which as a rule meet a constraint in the bed to carry away the heat generated and to maintain the optimal temperature in it.

It is known [1] that in the conditions realized in high-temperature fluidized beds the external heat transfer has a complex conductive–convective–radiative nature. Its intensity is influenced by a number of factors, to compute which is a complex scientific problem.

A. V. Lykov ITMO, Academy of Sciences of the Belorussian SSR, Minsk. I. I. Polnzuov NPO TsKTI, Leningrad.

Translated from Inzhenerno-Fizicheskii Zhurnal, Vol. 56, No. 5, pp. 767-773, May, 1989. Original article submitted December 14, 1987.

TABLE 1

Fuel flow rate, B_s, kg/h	600 — 1400
Static bed height H_0, mm	200 — 300
Air excess factor, α_f	1,34 — 2,0
Bed temperature, T_∞, K	1073 — 1273
Air velocity u, m/sec	1,8 — 4,57.

TABLE 2. Equivalent Diameters of the Test Dispersed Materials

d_1	d_2	Dispersed material
mm		
2,62	1,05	S.1
4,90	1,81	S.2
5,32	2,93	S.3
7,25	3,60	S.4
6,26	4,00	S.5

Prior to the poresent study we addressed the problem of elucidating the influence of the fractional composition of the bed material and its temperature on the intensity of heat transfer with the surrounding surface.

To analyze the complex heat transfer process we used the two-zone heat transfer model suggested earlier [2]. Postulating a gas layer transparent to radiation and assuming that the heat transfer in the developed fluidized bed is limited only by the resistance of the gas film at the heat transfer surface [2], we can write the system of equations describing the process in the following form (heat transfer with a vertical cylinder):

$$\frac{1}{r}\frac{d}{dr}\left(\lambda_f(T_f)\, r\frac{dT_f}{dr}\right) - \frac{c_f J (T_f - T_0)}{Hm} = 0, \tag{1}$$

$$T_f(a) = T_w;\ T_f(a + l_0) = T_\infty \tag{2}$$

with the added condition

$$-\lambda_f \frac{dT_f}{dr}\bigg|_{r=a+l_0} - \sigma^*(T_\infty^4 - T_w^4) = \frac{c_f J (T_\infty - T_0)}{H}\frac{R^2 - a^2}{2a}, \tag{3}$$

which defines the temperature of the incoming gas (T_0), for a given value of T_∞. The effective emissivity appearing in σ^* is given by the expression [3]

$$\varepsilon_e/\varepsilon_b = (1 - A)(T_w/T_\infty)^4 + A. \tag{4}$$

The coefficient A in Eq. (4) reflects the influence of local temperature variation of particles at the heat transfer surface on the radiant flux.

The system (1)-(3) was solved numerically. For this it was written in the dimensionless form:

$$\frac{1}{\xi}\frac{d}{d\xi}\left(\Lambda(\theta_f^k)\,\xi\frac{d\theta_f^k}{d\xi}\right) = \mathrm{Pe}\,\theta_f^k \quad (a/l_0 \leqslant \xi \leqslant 1 + a/l_0), \tag{5}$$

$$\theta_f^k(a/l_0) = 1;\ \theta_f^k(1 + a/l_0) = \theta_\infty. \tag{6}$$

The solution of Eqs. (5)-(6) was found by a method of establishment from the corresponding unsteady problem, which was approximated on the uniform grid $\hat{\omega}_{h\tau} = \{\xi_i - a/l_0 = ih,\ t_j = j\tau,\ i = \overline{1, N},\ N = 1/h,\ j = 1, 2, \ldots\}$ by an implicit difference scheme (here h is the step size in ξ, and τ is the step size in dimensionless "fictitious" time t). Since $\theta_f{}^k$ is a function of $T_0{}^k$, the solution of the system (5)-(6) is first found for the given initial approximation for the gas temperature $T_0{}^0$. Each successive $T_0{}^k$ required to determine $\theta_f{}^k$ from Eqs. (5)-(6) was computed from the condition, which follows from Eq. (3):

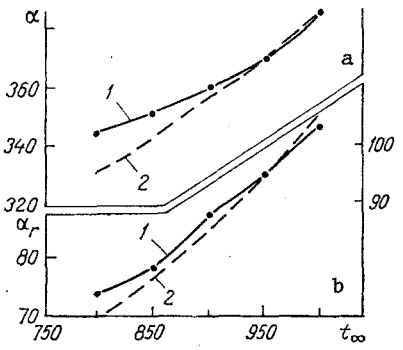

Fig. 1

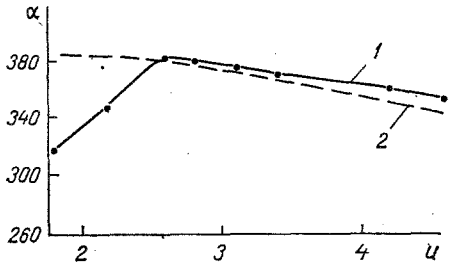

Fig. 2

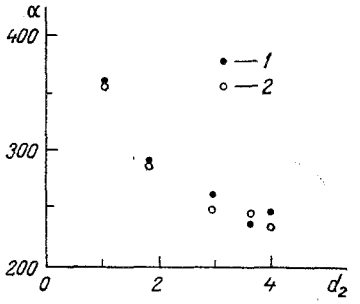

Fig. 3

Fig. 1. Dependence of the maximum heat transfer coefficient (a) and its radiative component (b) on the fluidized bed temperature. The bed material is S.1: 1) test data; 2) computed from Eq. (11). The quantities α, α_r are in W/(m²·K); t_∞ is in °C.

Fig. 2. Dependence of the heat-transfer coefficient on the filtration speed. The bed material is S.1. The symbols are the same as for Fig. 1. Here t_∞ = 1000°C, and u is in m/sec.

Fig. 3. Dependence of the maximum heat transfer coefficient on the equivalent diameter d_2. The symbols are the same as in Fig. 1. Here t_∞ = 900°C, and d_2 is in mm.

$$-\frac{\lambda_f(T_\infty)(T_w-T_0^{k-1})}{l_0}\frac{d\theta_f^{k-1}}{d\xi}-\sigma^*(T_\infty^4-T_w^4)=\frac{c_fJ(T_\infty-T_0^k)}{H}\frac{R^2-a^2}{2a}. \tag{7}$$

The iterative process of finding T_f^k and T_0^k ended when $(T_0^k - T_0^{k-1})/T_0^k| \le 10^{-5}$.

The calculations were made for d_1 = 2-6 mm; T_∞ = 873-1473 K; T_W = 873-1473 K. It was determined that the coefficient α defined from Eqs. (5) and (6) with the aid of the expression

$$\alpha=\frac{\lambda_f(T_f(a))}{T_\infty-T_w}\frac{dT_f(a)}{dr}+\frac{\sigma^*(T_\infty^4-T_w^4)}{T_\infty-T_w}, \tag{8}$$

coincides, to within 1%, with the value of α found by solving Eqs. (5) and (6) with Pe = 0 (for the firing conditions with a fluidized bed estimates show that the values of Pe do not exceed 0.4).

The results of the numerical experiment allow us to use the system (5) and (6) with Pe = 0 to analyze the laws of the complex heat transfer. With $\lambda_f = \lambda_f^0 + Bt_f$ it allows a simple analytical solution, which for $l_0/a \ll 1$ has the form [4]

$$t_f=-\lambda_f^0/B+\sqrt{\left(\frac{\lambda_f^0}{B}\right)^2+\frac{2}{B}\left(\frac{\lambda_f^0(t_\infty-t_w)+\frac{B}{2}(t_\infty^2-t_w^2)}{l_0}(r-a)+\lambda_f^0t_w+\frac{B}{2}t_w^2\right)}. \tag{9}$$

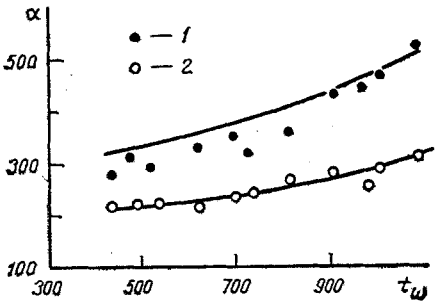

Fig. 4

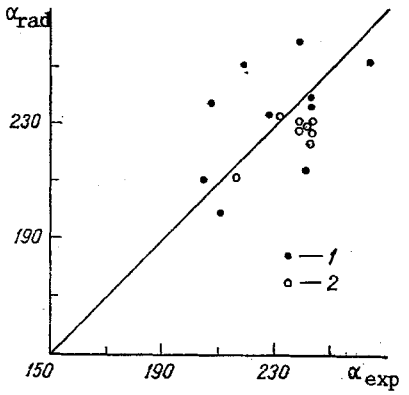

Fig. 5

Fig. 4. Dependence of the heat transfer coefficient on the surface temperature and surface emissivity: 1) $\varepsilon_w = 0.8$; 2) 0.20 [9]. The curves show values computed from Eq. (11). The dispersed material is alundum (d = 6 mm, $\varepsilon_s = 0.42$), $t_\infty = 1200°C$ and t_w is in °C.

Fig. 5. Comparison with the test data of [11] and [12]: 1) fire clay [11] ($d_1 = 1.47$ mm; $d_2 = 1.17$ mm); $T_w = 293$ K; $T_\infty = 873$-1073 K; 2) fire clay [12] ($d_2 = 1.8$ mm; $d_1 = 2.3$ mm); $T_w = 298$ K; $T_\infty = 985$-1116 K. The quantities α_{rad}, α_{exp} are in W/(m²·K).

The coefficient of the complex heat transfer, defined by Eqs. (8) and (9), can be expressed as follows:

$$\alpha = \frac{\langle \lambda_f^c \rangle}{l_0} + n\frac{c_f J d_2}{m l_0} + \sigma^*(T_\infty^2 + T_w^2)(T_\infty + T_w). \quad (10)$$

Using the expressions for ℓ_0 and n obtained in [2], we can write Eq. (10) in the form

$$\alpha = \frac{7{,}2\langle \lambda_f^c \rangle}{d_2}(1-m)^{2/3} + 0{,}044 c_f (\rho_f u)_{T_\infty}\frac{(1-m)^{2/3}}{m} + \sigma^*(T_\infty^2 + T_w^2)(T_\infty + T_w). \quad (11)$$

Equation (11) sets out the form of the functional dependence of the coefficient α on the governing factors and was used subsequently to correlate the test data.

To verify the relation obtained, Eq. (11), and to determine the coefficient A, accounting, as was noted above, for the influence of local particle temperature variation near the heat exchanger surface, special experiments were performed.

The heat transfer from a vertical tube of diameter 32 mm was studied in a reconstructed type DKVr6.5-13 industrial boiler of capacity 10 tons/h. The tests were made with Donets gas coal of size d = 1.5-8.5 mm (maximum size 20 mm). As the bed material we used ash of different fractional composition. The equivalent diameters of these dispersed materials are shown in Table 1. The experiments were conducted for the following conditions ($T_w = 303$ K).

The experimental technique to measure the heat flux was described in detail in [5]. The emissivities of the heat exchange surface and the bed particles were 0.8 and 0.7, respectively.

Figure 1 shows the test data on the measured values of α and α_r in bed material S.1 (see Table 2) for different bed temperatures T_∞. Figure 1 also shows the values, calculated from Eq. (11), of the total heat transfer coefficient and its radiative component. The mean porosity of the bed was determined from the formula [6]

$$m = m_0 + 1{,}56\,\frac{\mathrm{Re} - \mathrm{Re}_0}{\sqrt{\mathrm{Ar}}}(1 - m_0). \tag{12}$$

The emissivity of the isothermal fluidized bed was computed from the relation [7]

$$\varepsilon_b = 1{,}63\,\frac{m - m_0}{1 - m_0}\,\varepsilon_s^{0{,}310} + \left(1 - 1{,}63\,\frac{m - m_0}{1 - m_0}\right)\varepsilon_s^{0{,}485}. \tag{13}$$

It was established that the best agreement of the test and theoretical data on α_r is obtained with A = 1. This means that for large particles (d $\gg$ 1 mm) we can neglect cooling at the heat exchange surface. This agrees with the results of [8], where it was shown that the intense interphase heat transfer in beds of particles with d > 1 mm is compensated to a considerable degree by heat loss of the particles via conduction to the wall. Taking this into account, we put A = 1 subsequently in analyzing the test data with Eq. (11). We note here that in the case of small particles the supercooling at the heat transfer surface appreciably affects the radiative heat flux. For example, our analysis of the results of [1, 9] on measurement of the apparent emissivity of a fluidized bed of corundum particles (d = 0.32, 0.5 mm) has shown that in the bed temperature range T_∞ = 873-1498 K and $T_W \ll T_\infty$ the coefficient A varied in the range 0.58-0.43.

Figure 2 shows the dependence of the coefficient α on the speed of filtration of the gas for material S.1. A noticeable discrepancy between the test and the computed data is observed only for small speeds of filtration, when one should cease to use the assumption of perfect mixing of particles at the heat transfer surface.† Figure 3 shows the test values of α_{max} and those calculated from Eq. (11) for mixtures of different equivalent diameter. As can be seen, these also show quite satisfactory mutual agreement.

Figures 4 and 5 show the published data on the measurement of α in high-temperature fluidized beds and a comparison with values computed from Eq. (11). In all cases the maximum deviation of the test data from the calculated does not exceed 15%.

It should be stressed that in Eq. (11) the equivalent diameter $d_2 = 1/\Sigma(\eta_i/d_i)$ is used. However, to calculate the porosity of a fluidized bed from Eq. (12), one should use the equivalent diameter $d_1 = \Sigma\eta_i d_i$ (this diameter is used in determining u_0 [13]). An analogous situation occurs also with the determination of temperature. In Eq. (11) the coefficient λ_f^c is computed for $T = (T_\infty + T_W)/2$, while the values of gas density and filtration speed are evaluated at the bed core temperature T_∞. In Eq. (12) all the parameters are also computed at T_∞.

In conclusion, we note that the correlation obtained, Eq. (11), satisfactorily describes the available data on heat transfer in high-temperature beds of coarse polyfractionated particles. It takes account of the basic special features of heat transfer in such systems and can be used for engineering design of heat exchangers in beds of particles with d = 1-7 mm and temperature up to 1473 K.

NOTATION

a, tube radius; c_f, specific heat of the gas; $d_1 = \Sigma\eta_i d_i$; $d_2 = 1/\Sigma(\eta_i d_i)$; d_i, mean diameter of the i-th fraction; g, acceleration due to gravity; H, height of the fluidized bed; $J = \rho_f u$, mass flow rate of gas; ℓ_0, thickness of the gas film on the heat transfer surface; m_0, porosity at the onset of fluidization; m, porosity; r, radius; R, radius of the equipment; t_f, °C; T_f, °K, gas temperature; T_0, initial gas temperature; T_∞, T_W, temperature of the fluidized bed and of the heat transfer surface, u, u_0, speed of filtration and speed at the start of fluidization; α, heat-transfer coefficient; ε_W, ε_b, emissivities of the heat transfer surface, and the fluidized bed; ε_s, emissivity of the particles; ε_e, effective (apparent) emissivity of the fluidized bed; $\varepsilon^* = 1/(1/\varepsilon_W + 1/\varepsilon_e - 1)$; η_f, viscosity of the gas; $\theta_f = (T_f - T_0)/(T_W - T_0)$; λ_f, thermal conductivity of the gas; $\lambda_f^0 = \lambda_{f0}^c + nc_f J d_2/m$, thermal conductivity of the gas at t_f = 0°C; λ_f^c, molecular thermal conductivity of the gas; $\langle\lambda_f^c\rangle$, at temperature $(T_W + T_\infty)/2$; λ_{f0}^c, molecular thermal conductivity of the gas at t_f = 0°C, $\Lambda = \lambda_f/\lambda_{f0}^c$; $\xi = r/\ell_0$; ρ_S, ρ_f, density of particles in the gas; σ, Stefan–Boltzmann constant; $\sigma^* = \sigma\varepsilon^*$; $\mathrm{Ar} = gd_1^3\rho_f(\rho_S - \rho_f)/\eta_f^2$, Archimedes Number; $\mathrm{Pe} = c_f J\ell_0^2/\mathrm{Hm}\lambda_{f0}^c$, Peclet number; $\mathrm{Re} = ud_1\rho_f/\eta_f$, Reynolds Number; $\mathrm{Re}_0 = u_0 d_1\rho_f/\eta_f$.

†The assumption of perfect mixing in the bed core may remain valid here [10].

LITERATURE CITED

1. A. P. Baskakova (ed.), Heat and Mass Transfer Processes in a Fluidized Bed [in Russian], Moscow (1978).
2. V. A. Borodulya, V. L. Ganzha, Yu. S. Teplitskii, et al., Inzh.-Fiz. Zh., 49, No. 4, 621-626 (1985).
3. V. I. Kovenskii, "Modeling of radiative heat transfer in a fluidized bed," Authors Abstract of Candidate's Dissertation, Minsk (1981).
4. V. P. Isachenko, V. A. Osipova, and A. S. Sukomel, Heat Transfer [in Russian], Moscow (1981).
5. V. I. Antonovskii, V. V. Mantsnev, A. G. Grebenshchikov, et al., Development of Boiler Equipment for Operation on Low-Grade Solid Fuel, No. 191, 88-95, Leningrad (1981) (Tr. TsKTI im. I. I. Polzynov).
6. V. A. Borodulya, V. L. Ganzha, and V. I. Kovenskii, Hydrodynamics and Heat Transfer in a Fluidized Bed under Pressure [in Russian], Minsk (1982).
7. V. I. Kovenskii, Inzh.-Fiz. Zh., 38, No. 6, 983-988 (1980).
8. V. A. Borodulya and V. I. Kovenskii, Inzh.-Fiz. Zh., 47, No. 5, 789-796 (1984).
9. O. M. Panov, A. P. Baskakov, O. M. Goldobin, et al., Inzh.-Fiz. Zh., 36, No. 3, 409-415 (1979).
10. J. Botterill, Heat Transfer in the Fluidized Bed [Russian translation], Moscow (1980).
11. A. I. Tamarin, Yu. G. Epanov, I. S. Rassudov, et al., Énergomashinostroenie, No. 12, 7-8 (1977).
12. A. V. Ryzhakov, V. I. Babii, Yu. G. Pavlov, et al., Teploénergetika, No. 11, 31-35 (1980).
13. V. A. Borodulya, V. L. Ganzha, Yu. S. Teplitskii, et al., Fluidization of Polydispersed Beds of Coarse Particles [in Russian], Minsk (1984). (Preprint of Inst. Heat Mass Transfer, Acad. Nauk BSSR, No. 4).

COMPREHENSIVE DETERMINATION OF POTENTIAL-DEPENDENT HEAT- AND MASS-TRANSFER CHARACTERISTICS OF DISPERSE MATERIALS

S. V. Mishchenko and P. S. Belyaev

UDC 536.24.093:539.215.4

A method is proposed for parametric identification of a mathematical model of coupled heat and mass transfer (HMT) in a disperse medium.

The heat- and mass-transfer characteristics of disperse media generally depend on the temperature and concentration of the substances distributed in the solid phase, which makes it necessary to account for type I nonlinearity [1] in the corresponding inverse problems.

The methods and equipment that are developed should provide not only for comprehensive determination of the HMT characteristics of disperse media, but also for the solution of the more complicated problem – recording of the dependence of the sought characteristics on the temperature of the test material and the concentration of the substance distributed in it.

The analysis conducted in [2] showed that the methods and equipment currently used in laboratory practice for comprehensive determination of the HMT characteristics of disperse materials do not fully meet the above requirements and are in need of improvement. They are not sufficiently accurate and lack the proper theoretical and metrological underpinnings. Substantial methodological errors are introduced by the linear mathematical models (MM) used in place of nonlinear models and the simplifications made to nonlinear models in the derivation of the formulas. Another shortcoming of the methods is the need to measure temperature and local concentration at several points of the test specimen, which complicates the measuring equipment and diminishes its reliability.

Tambov Institute of Chemical Engineering. Translated from Inzhenerno-Fizicheskii Zhurnal, Vol. 56, No. 5, pp. 773-779, May, 1989. Original article submitted December 12, 1987.

 0022-0841/89/5605-0546$12.50